Desalination and Water Treatment
www.deswater.com
doi: 10.5004/dwt.2023.30198

316 (2023) 317–326
December

Preparation of Pb/biochar composite as particle electrode for three-dimensional electrochemical oxidation of chemical oxygen demand from chemical wastewater

Mingyue Piao[a,b], Jing Zhang[b], Huishi Du[c], Hongxue Du[a], Honghui Teng[a,b,*]

[a]*Key Laboratory of Environmental Materials and Pollution Control, Education Department of Jilin Province, Jilin Normal University, Siping, China, emails: tenghonghui@163.com (H. Teng), 2577246959@qq.com (M. Piao), duhongxue666@jlnu.edu.cn (H. Du)*
[b]*College of Engineering, Jilin Normal University, 1301 Haifeng Road, Siping 136000, China, email: zhangjing@jlnu.edu.cn*
[c]*College of Tourism and Geographical Science, Jilin Normal University, Siping, China, email: duhs@jlnu.edu.cn*

Received 31 August 2023; Accepted 3 December 2023

ABSTRACT

The use of three-dimensional (3D) electrochemical oxidation has become a popular method for treating water pollutants. In this study, the degradation of real wastewater discharged by the chemical industry was conducted using Pb loaded biochar (Pb/BC) as a particle electrode. The properties of Pb/BC were characterized by scanning electron microscopy, X-ray diffraction, energy-dispersive X-ray spectroscopy, Fourier-transform infrared spectroscopy, X-ray photoelectron spectroscopy, and Brunauer–Emmett–Teller. The impact of various factors, including Pb loading, pH, dosage of Pb/BC, and working voltage, on chemical oxygen demand (COD) elimination were examined, and the best results were obtained on pH 7 and working voltage of 14 V, with 25 g/L Pb/BC (8% Pb loaded on BC) added in 3D reaction system. The degradation process was well fitted with the first-order kinetic. COD removal efficiency was 67.60% after 90 min reaction with only 6.21 kW·h/kg_{COD} of energy consumption. The presence of tert-butanol had a significant impact on decreasing the efficiency of COD removal, suggesting that the hydroxyl radicals produced during the reaction were the primary means of degrading COD, rather than direct electro-oxidation. Toxic results indicated that the treated wastewater was less toxic than the original water. The use of Pb/BC may have practical applications in the treatment of actual chemical wastewater.

Keywords: Chemical wastewater; Chemical oxygen demand removal; Energy consumption; Three-dimensional electrocatalytic oxidation; Pb/biochar particle electrode

1. Introduction

Chemical wastewater is a major challenge in pollutant treatment as it is highly toxic and bio-refractory, posing a significant threat to the environment [1]. Electrochemical oxidation is an advanced oxidation process that has proven to be highly effective in degrading waste waters containing recalcitrant substances due to its strong oxidation capacity and high efficiency [2–5]. Unavoidably, electrochemical oxidation also has significant drawbacks, such as high energy consumption, the formation of by-products, and low energy efficiency. Addressing these issues remains a significant challenge that must be effectively resolved [6,7].

Compared to two-dimensional (2D) electrochemical oxidation, three-dimensional (3D) electrochemical oxidation typically exhibits superior performance in terms of treatment efficiency and energy consumption. This is due to the use of particle electrodes that fill the gap between positive and negative plate electrodes, can provide a larger contact surface and a higher electron-transport capability [8,9], thus it has been successfully applied for treating refractory waste waters, such as dye [10], coal chemistry [11], nitrobenzene

* Corresponding author.

[12], norfloxacin [13,14], landfill leachate [15], and phenol [16]. The type of particle electrode is crucial in determining treatment efficiency and cost-effectiveness. As a result, the development of high-performance particle electrodes has become increasingly important.

Biochar (BC) has been used extensively in recent years to remedy environmental pollution because it is inexpensive, environmentally acceptable, and readily available from a variety of sources with adsorption ability [17–19]. Being impregnated with mineral ions can enable BC to catalyze pollutants, along with changing its specific surface area, pore size, and/or pore volume [20–22]. Previous studies have attempted to improve electrochemical degradation efficiency of BC by combination with various metal oxides, including Fe [23], Fe/N [24], Ni [25], and CoAl-layered double hydroxide [26]. Currently, designing supported components remains the most effective method for enhancing the stability and catalytic activity of particle electrodes.

This study aims to explore the potential of using Pb/biochar (Pb/BC) as a particle electrode for electrochemical oxidation chemical wastewater. The structures and chemical properties of the particle electrodes were investigated, with a specific focus on the impact of various operating variables on chemical oxygen demand (COD) oxidation. These variables include Pb loading, pH, Pb/BC dosage, and working voltage. Finally, by optimizing the operational variables, the energy consumption and possible COD degradation ways were also proposed.

2. Materials and methods

2.1. Materials and chemicals

$Pb(NO_3)_2$, NaOH, HCl, $(NH_4)_2FeSO_4$, $K_2Cr_2O_7$, and C_2H_5OH were purchased from Aladdin Chemical Co., (China). All the chemicals used in this study were analytical reagent grade without further purification. Corn straw was collected from local farmland.

2.2. Preparation of Pb/BC particle electrode

Corn straw was selected as the raw material, and washed twice with distilled water to remove impurities. The material was dried in an oven at 80°C for 12 h, and then ground into powder. By hydrothermal method, BC was produced [27]. Pb modified BC particle electrode was prepared by an immersion–calcination method as following: pure BC was added into Pb^{2+} solution at a solid–liquid ratio of 1:20 g/mL and sonic for 2 h, then the solid substance was filtered out, followed by dried at 80°C for 48 h. Subsequently, it was calcined at 400°C for 2 h in an electric furnace. After cooling, it was washed several times with distilled water until it reached a constant pH, and then dried in an oven for 24 h. The obtained catalyst was named as Pb/BC.

2.3. Characterization of Pb/BC

The surface morphology and energy-dispersive X-ray spectroscopy (EDS) of Pb/BC was examined using a scanning electron microscopy (SEM) (XL30, FEI, USA) at a working voltage of 10 kV. The crystalline phase was characterized by X-ray diffraction (XRD; D/max-2500, Rigaku, Japan) in a range of $2\theta = 10°–80°$ with Cu-Kα radiation ($\lambda = 1.5406$ Å, 40 kV, 200 mA). After grinding and thoroughly mixing it with KBr powder, the powder mixture was compressed into a transparent disk. Then an Fourier-transform infrared spectroscopy (FTIR; Tensor 320, Bruker, German) was used to scan from 4,000 to 400 cm^{-1} using an average of 16 scans, with a resolution of 1 cm^{-1}. The chemical states were tested by X-ray photoelectron spectroscopy (XPS, ESCALAB 250, USA). At the N_2 adsorption and desorption analyzer, specific surface area, pore volume, and pore size were evaluated utilizing Brunauer–Emmett–Teller (BET) and Barrett–Joyner–Halenda calculation.

2.4. Electrochemical oxidation of real chemical wastewater

The wastewater sample was obtained from Jianxin Chemical Plant located in Hebei, China. To ensure consistency in the sample quality, it was stored at a temperature of 4°C in a deep freezer. The sample has a high concentration of COD (35,000 mg/L) and poor biodegradability ($BOD_5/COD_{Cr} < 0.13$) with suspended matter. The conductivity of the sample was measured to be 12.6 mS/cm, and the pH was approximately 7.2. In order to prevent the blockage of pores in the particle electrode by suspended matter, a pretreatment process was carried out. A certain amount of polyaluminum chloride and polyacrylamide was added into the wastewater and stirred slowly for 5 min until flocculation occurred. The solution was then left to stand for 30 min to allow for precipitation, after which it was filtered for use. Prior to electrochemical oxidation, an adsorption process was allowed to occur for a period of 90 min until equilibrium was reached. The electrocatalytic degradation was then conducted in a reactor measuring 8 cm × 6 cm × 21 cm and containing 0.4 L of chemical wastewater. The cathode and anode were made of 304 stainless steel plates and were parallel to each other with a gap of 2.5 cm. Additionally, Pb/BC particles were filled in to create a 3D electrochemical oxidation system.

2.5. Analytical methods

COD was measured using the standard dichromate method on the samples. The samples were refluxed at 150°C for 2 h and then allowed to cool to ambient temperature. The residual dichromate ions were titrated using $(NH_4)_2{\cdot}FeSO_4$ solution. Conductivity and pH were measured using a conductivity meter and a pH meter, respectively.

2.6. Toxic experiment

Randomly selected 2 h post fertilization (hpf) zebrafish embryos, and divided into 3 groups, including ultrapure water (control), original wastewater, and treated water. All groups include three parallel experiments. Each treatment contained 100 embryos and 30 mL of diluted exposure solution. The diluted exposure solutions were diluted tenfold and renewed every 48 h, and dead embryos were removed in time during the exposure experiment. The exposure was conducted in an illumination incubator at a temperature of 28°C with a photo period of 14:10 h (light:dark). The hatching and mortality rates were recorded at 96 and 72 hpf, respectively.

3. Results and discussions

3.1. Characterization of Pb/BC

In Fig. 1 SEM images of pure BC and Pb/BC composites are presented. The surface of pure BC appeared relatively smooth, although some pores and cracks were visible. Following catalyst loading, the surface of the catalyst became rough with noticeable pores. Both Fig. 1 and Table 1 present EDS data, which demonstrate the successful loading of Pb onto pure BC with a content of 7.16%. This result was slightly lower than the theoretical load amount of 8%.

In Fig. 2a the XRD patterns of different samples were presented. The raw BC spectrum was significantly different from that of the catalyst-loaded BC. The typical diffraction peak of the BC was observed at approximately 23.97° of 2θ, which was attributed to the carbon crystal plane (JCPDS card no. 22-1069). On the other hand, for Pb/BC, the diffraction peak located at 26.2° can be indexed to the (110) planes (JCPDS card no. 76-0564), indicating that PbO_2 was loaded [28]. The presence of functional groups on the adsorbent surface was identified through FTIR spectroscopy and the results are displayed in Fig. 2b. The analysis revealed the presence of O–H (3,428–3,365 cm^{-1}), C–H (2,913 cm^{-1}), C–O (1,610–1,567 cm^{-1}), and C–C (1,387–1,385 cm^{-1}) in both BC and Pb/BC [29]. The introduction of Pb do not alter the functional groups on BC.

The XPS spectra of Pb/BC are presented in Fig. 3, revealing the presence of C, O, and Pb elements with atomic percentage contents of 87.08%, 12.84%, and 0.08%, respectively (Table 2). The C 1s XPS spectrum in Fig. 3b exhibits two carbon bonds, namely C–O (286.9 eV) and C–C (284.8 eV). The O 1s spectrum in Fig. 3c displays peaks of C=O, C–O, and Pb–O at 401.2, 399.7, and 398.6 eV, respectively. Additionally, Fig. 3d shows the appearance of double peaks in the Pb 4f cleavage energy levels (f5, f7) [30], and the peak of PbO_2 (139.5 and 143.5 eV) and $PbCO_3$ (138.0 and 142.7 eV) can be observed, which indicated the generation of PbO_2 and $PbCO_3$ on the surface of BC [31,32]. As shown in Table 2, the atomic percentage of Pb^{4+} was 62.36%, and that was 37.64% for Pb^{2+}.

Table 3 presents the surface area and pore parameters obtained from the N_2 adsorption isotherms. The surface area, total pore volume, and pore diameter were determined to be 56.08 m^2/g, 0.4162 cm^3/g, and 2.06 nm, respectively. Upon catalyst loading, the surface areas were significantly increased to higher than 70 m^2/g, while the pore volume and diameter remained relatively unchanged.

Table 1
Energy-dispersive X-ray spectroscopy results of BC and Pb/BC

Sample	Element content (%)		
	C	O	Pb
BC	71.39	28.61	/
Pb/BC	66.28	26.56	7.16

3.2. Effect of working conditions on COD degradation

This study investigated the effect of varying Pb loading amounts on COD removal. Results showed that COD removal efficiency in 90 min increased with increasing Pb loading, reaching a maximum of 67.60% at 8% Pb loading. However, excessive Pb loading (15%) was found to inhibit COD removal, resulting in a lower efficiency of 53%. These findings suggested that while Pb loading can enhance COD removal, an optimal loading amount should be determined to achieve maximum efficiency. As Table 1 demonstrates, a decrease in surface area occurred when the Pb concentration exceeds 8%. This decrease in surface area subsequently led to a reduction in the amount of COD adsorbed on Pb/BC, potentially limiting the catalytic degradation of COD that follows.

The pH value is a crucial operational parameter in the electrochemical oxidation of organics. This is because, in most cases, the COD removal efficiency is highest at an optimum pH value. According to the findings in Fig. 4b, COD reduction increased with time from pH 3 to pH 7. However,

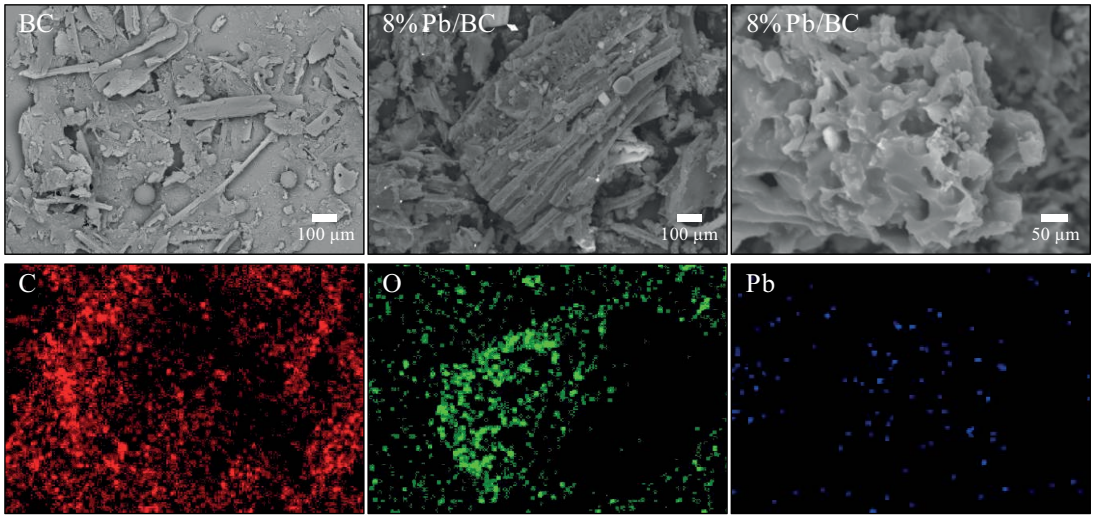

Fig. 1. Scanning electron microscopy and energy-dispersive X-ray spectroscopy images for Pb/BC.

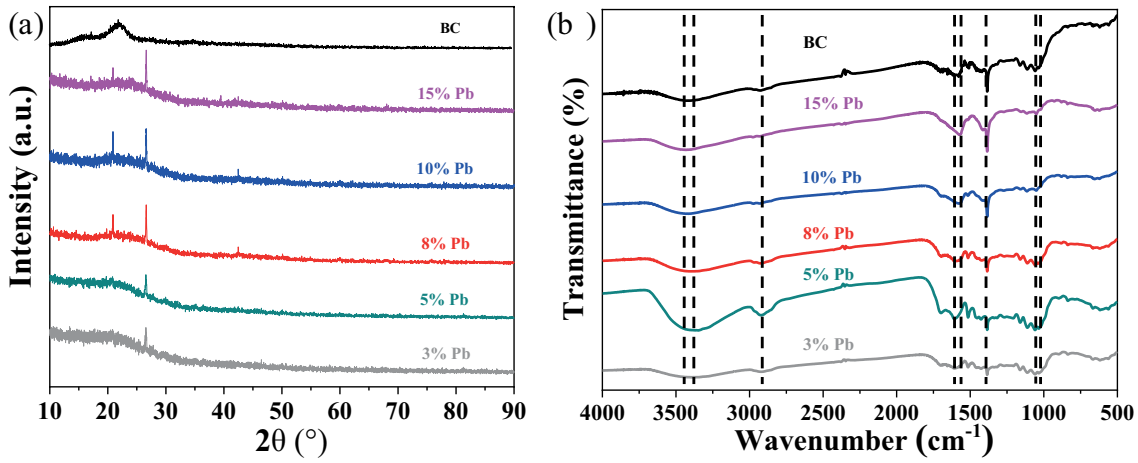

Fig. 2. Spectra of (a) X-ray diffraction and (b) Fourier-transform infrared spectroscopy of Pb/BC with different loading amount of Pb.

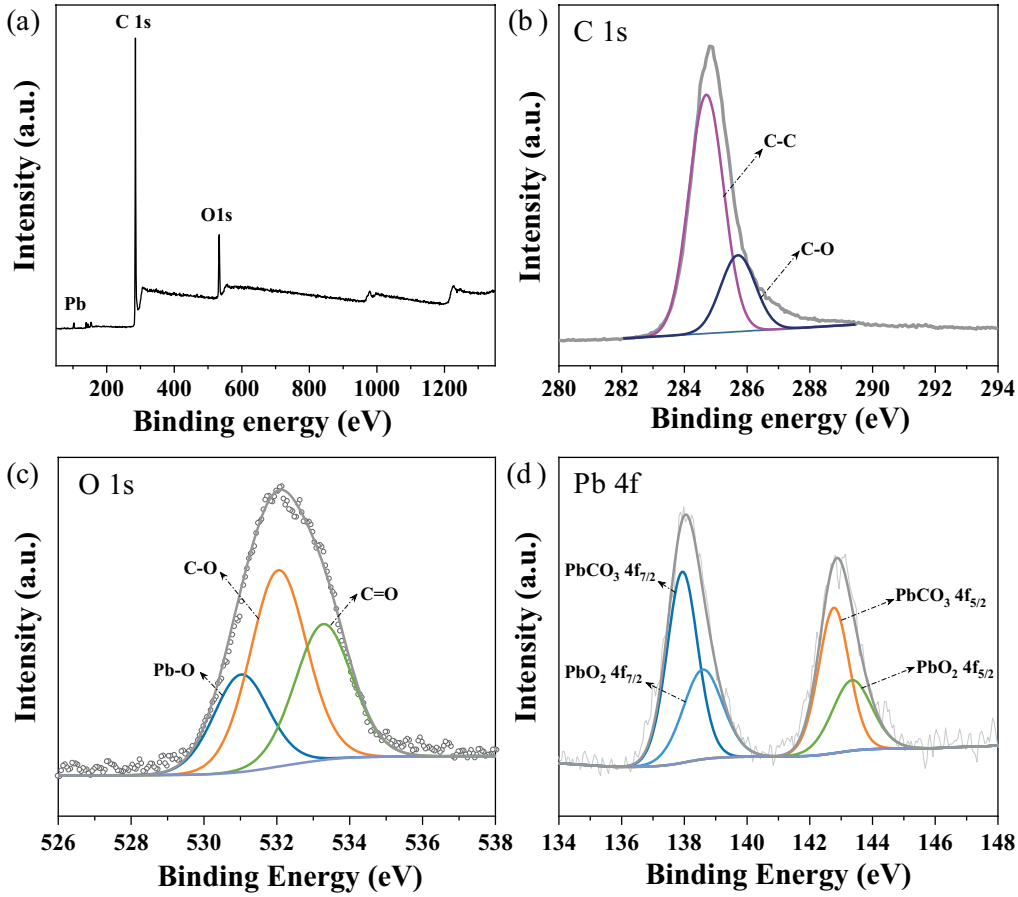

Fig. 3. X-ray photoelectron spectra of (a) full, (b) C, (c) O, and (d) Pb.

it decreased with further increase in pH up to 9. After 90 min, the following COD reductions were obtained: 46.8% at pH 3, 48.02% at pH 5, 67.6% at pH 7, and 50.95% at pH 9. In our study, a real-time decrease in pH levels within the system was observed. Specifically, when the initial pH was 7, the pH gradually decreased to 5.9 after 90 min, indicating a continuous production of H^+ during the electrolysis process. Two electrochemical and/or chemical processes may be responsible for the production of H^+: (1) the formation of hydroxyl radicals from water at the anode surface, which then react with organics in the diffusion layer; (2) the production of strong oxidizing species through the oxidation of inorganic ions at the anode surface, which then react with organics in the bulk solution [33].This study showed that

Table 2
Atomic percentage by X-ray photoelectron spectroscopy analysis

Name	Peak BE	Atomic (%)
C	284.80	87.08
O	532.62	12.84
Pb	139.08	0.08
Pb^{4+} $4f_{7/2}$	137.94	62.36
Pb^{4+} $4f_{5/2}$	142.77	
Pb^{2+} $4f_{7/2}$	138.59	37.64
Pb^{2+} $4f_{5/2}$	143.35	

Table 3
Brunauer–Emmett–Teller surface area and pore parameters of different samples

Sample	Surface area (m^2/g)	V (cm^3/g)	D (nm)
Pure BC	56.08	0.4162	2.06
3% Pb/BC	73.81	0.4265	2.20
5% Pb/BC	72.86	0.4238	2.16
8% Pb/BC	73.69	0.4289	2.14
10% Pb/BC	71.81	0.4001	2.15
15% Pb/BC	72.08	0.4002	2.15

the chemical wastewater can be treated without the need for pH adjustment, resulting in a reduction in running costs. This finding was consistent with Jia et al. [16] research, who examined the impact of pH levels (3, 5, 6.6, and 8) on phenol removal. They found that Sn-Mn-Ce-supported granular activated carbon (AC) was effective in breaking down phenol at a pH level of 6.6.

The results depicted in Fig. 4c indicate that the optimal Pb/BC dosage leads to effective COD removal. Specifically, a Pb/BC dosage of 25 g/L resulted in the highest COD removal efficiency (approximately 67.60%) within 90 min. However, at higher concentrations of Pb/BC (above 50 g/L), the current efficiency was decreased due to stronger bypass current, and thus the removal efficiency was decreased.

Working voltage is also an important parameter influencing removal efficiency of COD. As shown in Fig. 4d, it was approximately 49.98% at 12.0 V after 90 min, and the maximum value was achieved at 14 V. As the working voltage increased further, the COD removal efficiency gradually decreased. At 20 V, it was only about 53.02%. Although the 3D electrochemical reactor exhibits an increase in electric field intensity and particle polarization with the increase of the applied voltage, it may also lead to more noticeable side reactions. This, in turn, can decrease current utilization efficiency and has a negative impact on the degradation of organic compounds.

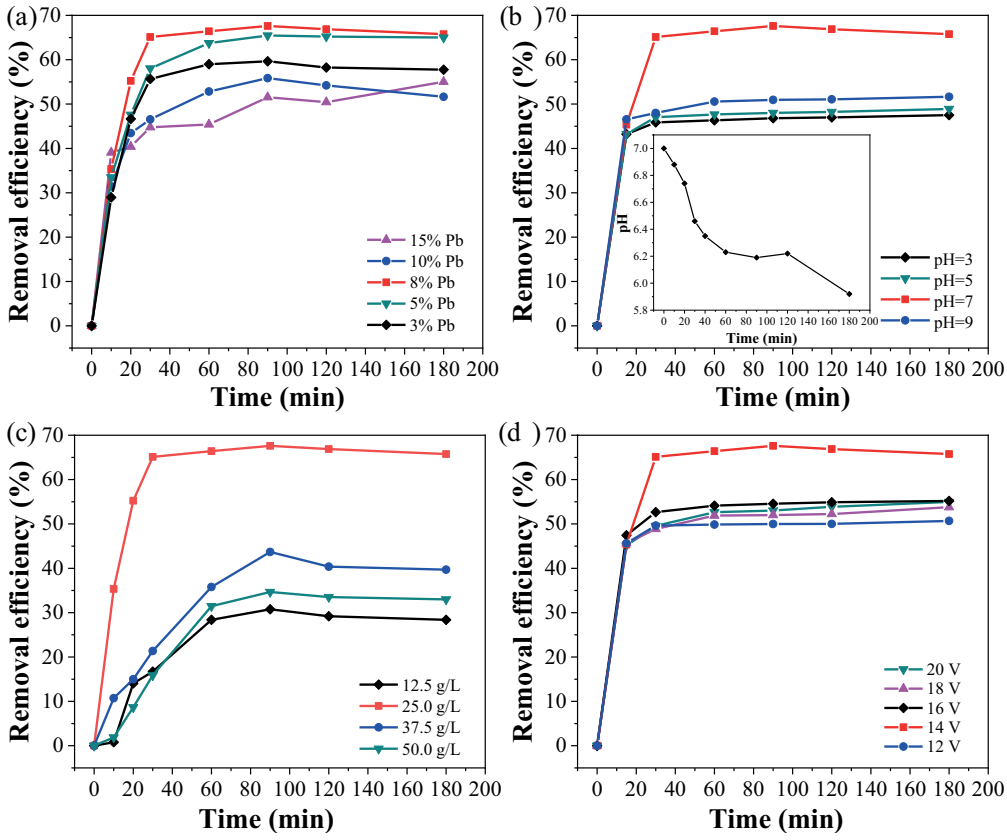

Fig. 4. Effect of (a) Pb loading amount, (b) pH (inset: pH changes during chemical oxygen demand removal at initial pH 7), (c) Pb/BC dosage, and (d) working voltage on chemical oxygen demand removal in 3D system.

To investigate the kinetic characteristics, the first-order model was utilized to analyze COD removal process. Both Table 4 and Fig. 5 showed that all reactions, regardless of Pb loading, following the first-order reaction dynamic model. The rate constants of oxidation using Pb/BC were 0.3672, 0.4122, 0.5670, 0.3474, and 0.3216 h^{-1} for Pb loadings of 3%, 5%, 8%, 10%, and 15%, respectively. The results were consistent with the degradation experiments as illustrated in Fig. 4a, confirming that the composite containing 8% Pb exhibited the best catalytic activity compared to other composites.

3.3. Energy consumption during COD degradation in 3D system

In Fig. 6a it is observed that COD removal efficiency for pure BC was 34.34% in 90 min, while Pb/BC with 8% Pb loaded on BC showed a higher efficiency of 67.6%. Moreover, the degradation rate of COD was faster with Pb/BC than with BC, indicating that Pb loading on BC could effectively improve COD removal. This is because each particle can be acted as a micro-electrolytic cell, with the formation of polarized micro-electrodes. When assessing the feasibility of wastewater treatment for larger-scale applications, energy consumption is a significant consideration. The specific energy consumption (E) is calculated using the following equation:

$$E = U \times I \times \frac{t}{\left(\mathrm{COD}_0 - \mathrm{COD}_t\right) \times V} \times 10^3$$

where E (kW·h/kg_{COD}) is energy consumption, U (V) is the working voltage, I (A) is the current intensity, t (h) is reaction time, V (L) is the volume of the chemical wastewater, COD_0 and COD_t (mg/L) are the concentration before and after electrochemical oxidation, respectively.

Table 5 shows that in a 90 min treatment, the removal efficiency and energy consumption were 67.6% and 6.21 kW·h/kg_{COD}, respectively. However, when using pure BC as a particle electrode, the removal efficiency and energy consumption were 34.34% and 15.28 kW·h/kg_{COD}, respectively. When Pb was loaded, the catalyst's active centers and hole sites were increased, resulting in a beneficial transformation of O_2 into strong oxidizing active components on the particle electrode. Furthermore, the presence of Pb, which contains the 4f orbital, may alter the energy level distribution of PbO_2 and increase the energy level states of the catalysts, resulting in enhanced catalytic activity and oxygen storage capacity of the particle electrode. Additionally, Pb/BC can absorb 24.19% of COD, indicating that the Pb/BC first adsorb COD and then electrochemical degrade it. Our results were compared to previous studies that reported on COD removal and/or corresponding energy consumption, despite differences in experimental conditions. Our findings,

Table 4
First-order kinetic parameters of chemical oxygen demand degradation in 3D system

Pb loading amount	k (h^{-1})	R^2
3%	0.3672	0.9518
5%	0.4122	0.8928
8%	0.567	0.9678
10%	0.3474	0.9548
15%	0.3216	0.9939

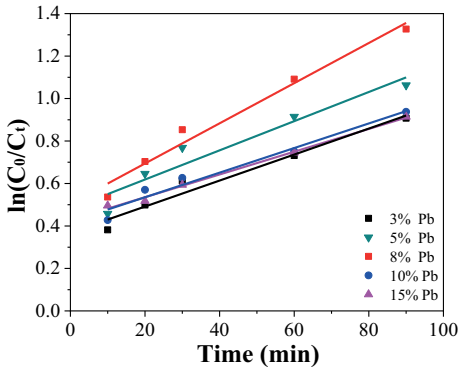

Fig. 5. The lnC–t curve of chemical oxygen demand degradation by Pb/BC with different Pb loading.

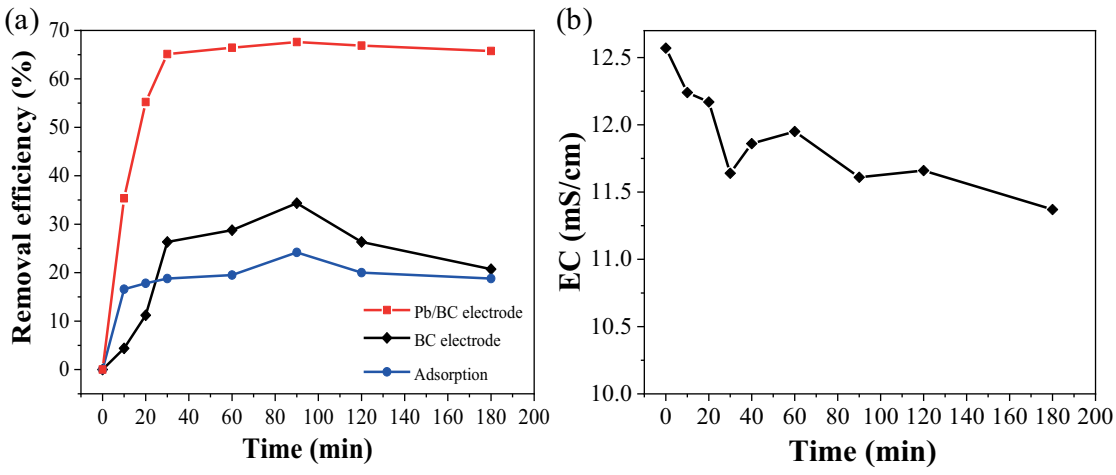

Fig. 6. Effect of (a) particle electrode and (b) conductivity change during reaction in 3D system.

Table 5
Energy consumption during chemical oxygen demand electrochemical oxidation

Particle electrode	E (kW·h/kg$_{COD}$)	Removal efficiency (%)	U (V)	I (A)	t (min)
BC	15.28	34.34	14	0.35	90
Pb/BC	6.21	67.60	14	0.28	90

Table 6
Energy consumption reported by previous works

Reaction system	E (kW·h/kg$_{COD}$)	Removal efficiency of COD (%)	Particle electrode	pH	Wastewater	t (min)	References
3D	/	87.5	Iron-loaded needle coke spherical electrodes	2.62	Real coking wastewater	360	[34]
3D	/	80	Ni/algal BC	3	Real electronic industry wastewater	60	[25]
2D	11.12	100	/	2.0	Real textile wastewater	180	[33]
2D	11.4	84	/	6.0	Real sugar industry wastewater	120	[35]
3D	13.5	56.9	AC	6.6	Simulated phenol wastewater	90	[16]
3D	7.6	75.6	Sn–Mn–Ce/AC	6.6	Simulated phenol wastewater	90	[16]
3D	80	80	Carbon black/polytetrafluoroethylene composite	4.0	Simulated phenol wastewater	120	[36]
3D	15.28	34.34	BC	7	Real chemical wastewater	90	This work
3D	6.21	67.6	Pb/BC	7	Real chemical wastewater	90	This work

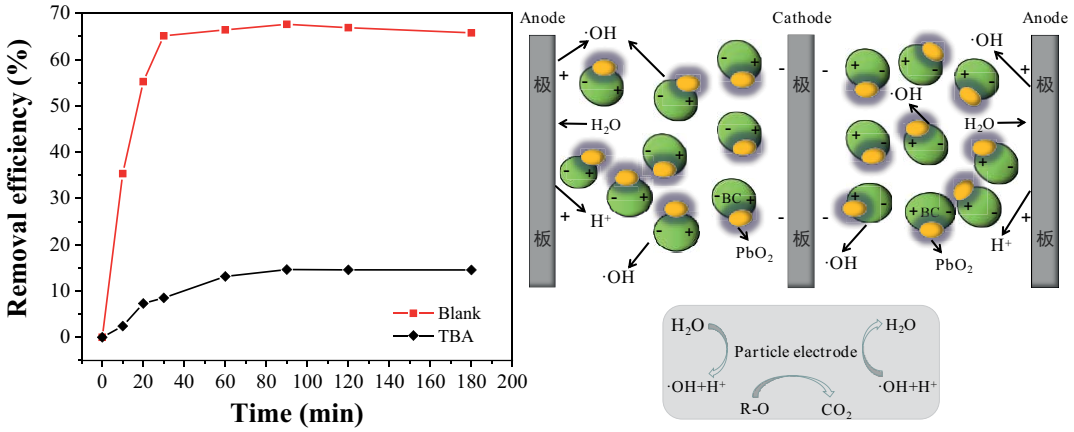

Fig. 7. (a) Effect of tert-butyl alcohol on chemical oxygen demand removal efficiency and (b) degradation mechanism.

presented in Table 6, demonstrate that Pb/BC particle electrodes have the potential to be a cost-effective solution for organic-compound degradation in 3D electrochemical oxidation. Fig. 6b shows that during COD reduction, the conductivity of the wastewater decreased, indicating that the electrochemical reaction can reduce free ions in the 3D system and therefore lowered conductivity.

3.4. Degradation mechanism

A quenching test was performed using tert-butyl alcohol (TBA) as radical scavengers. The results, as shown in Fig. 7a, indicate that the degradation efficiency of COD significantly decreased from 67.60% to 14.63% after introducing TBA into the 3D electrode system. This is because TBA may inhibit the hydroxyl radical in the system, which prevents it from participating in the electrochemical reaction. It was noteworthy that COD was still removed even after TBA addition, indicating that direct oxidation occurred. The electrochemical oxidation of organics in a 3D system occurs through two possible mechanisms: direct electron transfer from the anode to the organics, and oxidation mediated by hydroxyl radicals that produced near the anodic surface. The degradation mechanism is schemed as Fig. 7b.

3.5. Toxicity assessment

We investigated the toxic effects of the original wastewater and treated water on zebrafish. Zebrafish embryos of 2 hpf were exposed to the above solution for 96 h, and

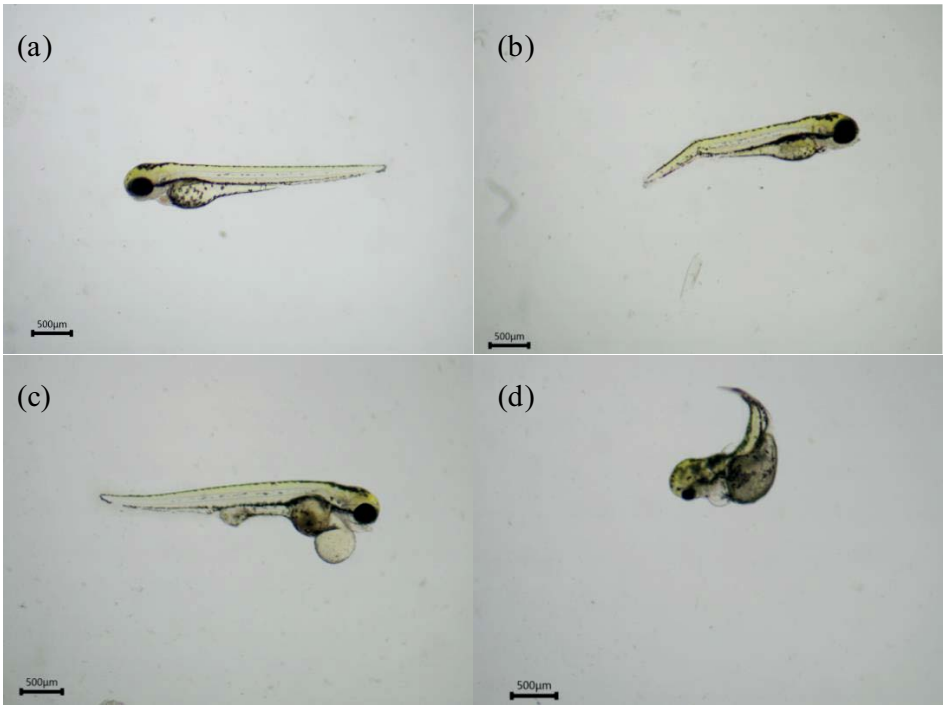

Fig. 8. (a) Normal larvae of the control group at 96 hpf. Malformation larvae of the test group including (b) spinal curvature, (c) pericardial oedema, and (d) co-occurrences at 96 hpf.

Table 7
Zebrafish hatching rate at 96 hpf and mortality rate at 72 hpf

	Blank		Treated water		Original wastewater	
	Value	σ	Value	σ	Value	σ
Mortality rate	12.67	2.06	13.00	2.45	74.67	11.32
Hatching rate	86.67	2.49	84.67	2.62	24.67	11.67

the toxicity changes were analyzed. As shown in Fig. 8a–d, the malformations of zebrafish (96 hpf) in original water, including pericardial oedema and spinal curvature, were recorded under a stereomicroscope. The zebrafish hatching rate at 96 hpf and mortality rate at 72 hpf are provided in Table 7. The hatched embryos in the blank group was 86.67%, while it was decreased slightly in the treated groups (84.67%) but decreased significantly in the original groups (24.67%). The mortality rate at 72 hpf was 12.67%, 13.00%, and 74.67% for blank, treated water, and original water, respectively. These results indicated that the treated wastewater was less toxic than the original water.

4. Conclusion

This study designed a 3D electrochemical oxidation reactor that utilizes Pb/BC as particle electrode to effectively degrade chemical wastewater. The Pb/BC composite was prepared using the coprecipitation–calcination method and characterized through various methods such as SEM, EDS, XRD, FTIR, XPS, and BET. For the 3D reactor with Pb/BC particle electrode, the most favorable results were observed under neutrality conditions at a working voltage of 14 V with the addition of 25 g/L of 8% Pb/BC. The degradation process was well-suited to the first-order kinetic model. COD removal efficiency and energy consumption were 67.60% and 6.21 kW·h/kg_{COD}, respectively. Additionally, the conductivity in wastewater decreased after electrochemical oxidation. The hydroxyl radicals produced during the reaction were the primary means of mineralization, rather than direct electro-oxidation. Toxic results indicated that the treated wastewater was less toxic than the original water.

Declarations

Ethics approval and consent to participate.
Not applicable.

Consent for publication

Not applicable.

Availability of data and materials

Not applicable.

Competing interests

The authors declare that they have no known competing financial interests or personal relationships that could have appeared to influence the work reported in this paper.

Funding

This work was supported by Education Department of Jilin Province of China (JJKH20230518KJ, JJKH20240575KJ), and Department of Science and Technology of Jilin Province of China (20210101398JC).

Author contribution

Mingyue Piao (writing and funding acquisition), Jing Zhang (investigation), Huishi Du (funding acquisition), Hongxue Du (investigation and funding acquisition), Honghui Teng (supervision).

References

[1] R. Zhou, S. Lu, Y. Su, T.T. Li, T.G. Ma, H.J. Ren, Hierarchically fusiform CuO microstructures decorated with Fe_3O_4 nanoparticles as novel persulfate activators for 4-aminobenzenesulfonic acid degradation in aqueous solutions, J. Alloys Compd., 815 (2020) 152394, doi: 10.1016/j.jallcom.2019.152394.

[2] M. Veciana, J. Bräunig, A. Farhat, M.-L. Pype, S. Freguia, G. Carvalho, J. Keller, P. Ledezma, Electrochemical oxidation processes for PFAS removal from contaminated water and wastewater: fundamentals, gaps and opportunities towards practical implementation, J. Hazard. Mater., 434 (2022) 128886, doi: 10.1016/j.jhazmat.2022.128886.

[3] M. Panizza, G. Cerisola, Removal of colour and COD from wastewater containing Acid Blue 22 by electrochemical oxidation, J. Hazard. Mater., 153 (2008) 83, doi: 10.1016/j.jhazmat.2007.08.023.

[4] J.Q. Bu, Z.W. Deng, H. Liu, T.H. Li, Y.J. Yang, S.A. Zhong, The degradation of sulfamilamide wastewater by three-dimensional electrocatalytic oxidation system composed of activated carbon bimetallic particle electrode, J. Cleaner Prod., 324 (2021) 129256, doi: 10.1016/j.jclepro.2021.129256.

[5] Z.W. Jiang, Y.C. Wang, H. Yu, N. Yao, J.H. Shen, Y. Li, H. Zhang, X. Bai, Efficient degradation of N-nitrosopyrrolidine using CoFe-LDH/AC particle electrode via heterogeneous Fenton-like reaction, Chemosphere, 313 (2023) 137446, doi: 10.1016/j.chemosphere.2022.137446.

[6] J. Qiao, Y.Z. Xiong, Electrochemical oxidation technology: a review of its application in high-efficiency treatment of wastewater containing persistent organic pollutants, J. Water Process Eng., 44 (2021) 102308, doi: 10.1016/j.jwpe.2021.102308.

[7] R. Fu, P.S. Zhang, Y.X. Jiang, L. Sun, X.H. Sun, Wastewater treatment by anodic oxidation in electrochemical advanced oxidation process: advance in mechanism, direct and indirect oxidation detection methods, Chemosphere, 311 (2023) 136993, doi: 10.1016/j.chemosphere.2022.136993.

[8] X. Wang, Z.L. Zhao, H.J. Wang, F. Wang, W.Y. Dong, Decomplexation of Cu-1-hydroxyethylidene-1,1-diphosphonic acid by a three-dimensional electrolysis system with activated biochar as particle electrodes, J. Environ. Sci., 124 (2023) 630, doi: 10.1016/j.jes.2021.11.036.

[9] N.N. Wang, L.W. Li, W.H. Zou, P. Wang, Performance and working mechanism of a coal fly ash-based particle electrode in the catalytic oxidation of ofloxacin in a three-dimensional electro-Fenton reactor, J. Environ. Chem. Eng., 11 (2023) 109561, doi: 10.1016/j.jece.2023.109561.

[10] R. Shokoohi, D. Nematollahi, M.R. Samarghandi, G. Azarian, Z. Latifi, Optimization of three-dimensional electrochemical process for degradation of methylene blue from aqueous environments using central composite design, Environ. Technol. Innovation, 18 (2020) 100711, doi: 10.1016/j.eti.2020.100711.

[11] W.Q. Sun, S.B. Zhou, Y.J. Sun, Y.H. Xu, H.L. Zheng, W-Ag-Ti@γ-Al_2O_3 particle electrodes for enhanced electrocatalytic pretreatment of coal chemical wastewater, J. Environ. Chem. Eng., 9 (2021) 104681, doi: 10.1016/j.jece.2020.104681.

[12] T. Wang, Y.Q. Song, H.J. Ding, Z. Liu, A. Baldwin, I. Wong, H. Li, C. Zhao, Insight into synergies between ozone and in-situ regenerated granular activated carbon particle electrodes in a three-dimensional electrochemical reactor for highly efficient nitrobenzene degradation, Chem. Eng. J., 394 (2020) 124852, doi: 10.1016/j.cej.2020.124852.

[13] Z.Y. Wang, B. Song, J.F. Li, X.L. Teng, Degradation of norfloxacin wastewater using kaolin/steel slag particle electrodes: performance, mechanism and pathway, Chemosphere, 270 (2021) 128652, doi: 10.1016/j.chemosphere.2020.128652.

[14] T. Wang, M.M. Ta, J. Guo, L.E. Liang, C. Bai, J. Zhang, H.J. Ding, Insight into the synergy between rice shell biochar particle electrodes and peroxymonosulfate in a three-dimensional electrochemical reactor for norfloxacin degradation, Sep. Purif. Technol., 304 (2023) 122354, doi: 10.1016/j.seppur.2022.122354.

[15] P. Asaithambi, R. Govindarajan, M.B. Yesuf, E. Alemayehu, Removal of color, COD and determination of power consumption from landfill leachate wastewater using an electrochemical advanced oxidation processes, Sep. Purif. Technol., 233 (2020) 115935, doi: 10.1016/j.seppur.2019.115935.

[16] Z.Z. Jia, X. Zhao, C.Y. Yu, Q. Wan, Y.F. Liu, Design and properties of Sn–Mn–Ce supported activated carbon composite as particle electrode for three-dimensionally electrochemical degradation of phenol, Environ. Technol. Innovation, 23 (2021) 101554, doi: 10.1016/j.eti.2021.101554.

[17] F. Amalina, S. Krishnan, A.W. Zularisam, M. Nasrullah, Recent advancement and applications of biochar technology as a multifunctional component towards sustainable environment, Environ. Dev., 46 (2023) 100819, doi: 10.1016/j.envdev.2023.100819.

[18] R. Kumar Mishra, D. Jaya Prasanna Kumar, A. Narula, S. Minnat Chistie, S. Ullhas Naik, Production and beneficial impact of biochar for environmental application: a review on types of feedstocks, chemical compositions, operating parameters, techno-economic study, and life cycle assessment, Fuel, 343 (2023) 127968, doi: 10.1016/j.fuel.2023.127968.

[19] S. Rawat, C.-T. Wang, C.-H. Lay, S. Hotha, T. Bhaskar, Sustainable biochar for advanced electrochemical/energy storage applications, J. Energy Storage, 63 (2023) 107115, doi: 10.1016/j.est.2023.107115.

[20] Q.K. Shi, S. Deng, Y.L. Zheng, Y.L. Du, L. Li, S.Z. Yang, G.X. Zhang, L. Du, G.F. Wang, M. Cheng, Y. Liu, The application of transition metal-modified biochar in sulfate radical based advanced oxidation processes, Environ. Res., 212 (2022) 113340, doi: 10.1016/j.envres.2022.113340.

[21] I.S. Marques, B. Jarrais, R. Ramos, V.K. Abdelkader-Fernandez, A. Yaremchenko, C. Freire, D.M. Fernandes, A.F. Peixoto, Nitrogen-doped biochar-supported metal catalysts: high efficiency in both catalytic transfer hydrogenation of furfural and electrocatalytic oxygen reactions, Catal. Today, 418 (2023) 114080, doi: 10.1016/j.cattod.2023.114080.

[22] Y.Z. Chai, M. Bai, A.W. Chen, X.Y. Xu, Z.H. Tong, J.Y. Yuan, L. Peng, J.H. Shao, J.H. Xiong, C. Peng, Upcycling contaminated biomass into metal-supported heterogeneous catalyst for electro-Fenton degradation of thiamethoxam: preparation, mechanisms, and implications, Chem. Eng. J., 453 (2023) 139814, doi: 10.1016/j.cej.2022.139814.

[23] L.H. Liu, R.H. Yu, S.X. Zhao, X.F. Cao, X.H. Zhang, S.Y. Bai, Heterogeneous Fenton system driven by iron-loaded sludge biochar for sulfamethoxazole-containing wastewater treatment, J. Environ. Manage., 335 (2023) 117576, doi: 10.1016/j.jenvman.2023.117576.

[24] Z.L. Yin, J.W. Zhu, Z.R. Wang, Y.L. Liu, Z. Yang, W.B. Yang, Novel Fe/N co-doping biochar based electro-Fenton catalytic membrane enabling enhanced tetracycline removal and self-cleaning performance, J. Cleaner Prod., 402 (2023) 136731, doi: 10.1016/j.jclepro.2023.136731.

[25] F. Guo, Y.Y. Lou, Q. Yan, J.L. Xiong, J.H. Luo, C.K. Shen, D.V. Vayenas, Insight into the Fe-Ni/biochar composite supported three-dimensional electro-Fenton removal of electronic industry wastewater, J. Environ. Manage., 325 (2023) 116466, doi: 10.1016/j.jenvman.2022.116466.

[26] X. Zhang, X.D. Zhang, C.J. An, S.G. Wang, Electrochemistry-enhanced peroxymonosulfate activation by CoAl-LDH@ biochar for simultaneous treatment of heavy metals and PAHs, Sep. Purif. Technol., 311 (2023) 123341, doi: 10.1016/j.seppur.2023.123341.
[27] S. Safarian, Performance analysis of sustainable technologies for biochar production: a comprehensive review, Energy Rep., 9 (2023) 4574, doi: 10.1016/j.egyr.2023.03.111.
[28] H.B. Han, J.H. Lyu, L.Y. Zhu, G.W. Wang, C. Ma, H.C. Ma, Fabrication of BN modified Ti/PbO_2 electrodes with tunable hydrophobic characteristics and their electrocatalytic performance, J. Alloys Compd., 828 (2020) 154049, doi: 10.1016/j.jallcom.2020.154049.
[29] H.S. Lee, H.S. Shin, Competitive adsorption of heavy metals onto modified biochars: comparison of biochar properties and modification methods, J. Environ. Manage., 299 (2021) 113651, doi: 10.1016/j.jenvman.2021.113651.
[30] W. Lin, W. Lo, J. Li, Y. Wang, J. Tang, Z. Fong, *In-situ* XPS investigation of the X-ray-triggered decomposition of perovskites in ultrahigh vacuum condition, npj Mater. Degrad., 5 (2021), doi: 10.1038/s41529-021-00162-9.
[31] J.Y. Wang, M. Xu, X. Liang, Y. Zhang, D.D. Yang, L. Pan, W.Y. Fang, C.G. Zhu, F.W. Wang, Development of a novel 2D Ni-MOF derived NiO@C nanosheet arrays modified Ti/TiO_2NTs/PbO_2 electrode for efficient electrochemical degradation of salicylic acid wastewater, Sep. Purif. Technol., 263 (2021) 118368, doi: 10.1016/j.seppur.2021.118368.
[32] K.D. Zhu, X.R. Wang, J. Zhong, S.L. Wang, Hydro-thermal preparation of $PbCO_3$/N-rGO nano-composites as positive additives to improve the performance of lead-acid batteries, J. Energy Storage, 53 (2022) 105102, doi: 10.1016/j.est.2022.105102.
[33] J.X. Zou, X.L. Peng, M. Li, Y. Xiong, B. Wang, F.Q. Dong, B. Wang, Electrochemical oxidation of COD from real textile wastewaters: kinetic study and energy consumption, Chemosphere, 171 (2017) 332, doi: 10.1016/j.chemosphere.2016.12.065.
[34] Y. Hu, F.Z. Yu, Z.T. Bai, Y.Q. Wang, H. Zhang, X.Y. Gao, Y.X. Wang, X. Li, Preparation of Fe-loaded needle coke particle electrodes and utilisation in three-dimensional electro-Fenton oxidation of coking wastewater, Chemosphere, 308 (2022) 136544, doi: 10.1016/j.chemosphere.2022.136544.
[35] O.P. Sahu, P.K. Chaudhari, Electrochemical treatment of sugar industry wastewater: COD and color removal, J. Electroanal. Chem., 739 (2015) 122, doi: 10.1016/j.jelechem.2014.11.037.
[36] H.J. Xiao, Y.J. Hao, J.L. Wu, X.Z. Meng, F. Feng, F.Q. Xu, S.Y. Luo, B. Jiang, Differentiating the reaction mechanism of three-dimensionally electrocatalytic system packed with different particle electrodes: electro-oxidation versus electro-Fenton, Chemosphere, 325 (2023) 138423, doi: 10.1016/j.chemosphere.2023.138423.